

Coarse-graining master equation for periodically driven systems

Ronja Hotz¹ and Gernot Schaller^{1,2*}

¹ *Institut für Theoretische Physik, Technische Universität Berlin,
Hardenbergstr. 36, 10623 Berlin, Germany and*

² *Helmholtz-Zentrum Dresden-Rossendorf, Bautzner Landstraße 400, 01328 Dresden, Germany*
(Dated: December 23, 2024)

We analyze Lindblad-Gorini-Kossakowski-Sudarshan-type generators for selected periodically driven open quantum systems. All these generators can be obtained by temporal coarse-graining procedures, and we compare different coarse-graining schemes. Similar to for undriven systems, we find that a dynamically adapted coarse-graining time, effectively yielding non-Markovian dynamics by interpolating through a series of different but individually Markovian solutions, yields the best results among the different coarse-graining schemes, albeit at highest computational cost.

I. INTRODUCTION

While the propagation of undriven closed quantum systems via Schrödingers equation may be challenging for many degrees of freedom, it can be calculated with standard methods. This changes when the Hamiltonian is subject to an external driving, when time-ordering becomes relevant. Even for the simple case of periodic driving, where Floquet theory [1, 2] applies, the exact calculation of the unitary propagator may be notoriously difficult [3–5]. In addition, it is then often hidden that the time-dependent variation of external parameters requires that the system is coupled in some way to an outside world, which to be complete would actually require to model the system as open. While open quantum systems in absence of driving are well-studied and interesting-subject on their own [6–8], the joint discussion of the effects of system-reservoir coupling and periodic driving is challenging.

However, with in particular periodic types of driving being experimentally quite feasible with current standards [9–13], the derivation of proper dissipators for periodically driven open systems is of great concern. In principle, it is formally possible to perform the same approximations that lead to Lindblad-Gorini-Kossakowski-Sudarshan (LGKS) master equations [14, 15] for an undriven system also for its driven version [3, 16–19]. In the interaction picture, the application of Born-, Markov-, and secular approximations generically leads to LGKS master equations that come handy due to their stability and – despite the lack of thermalization [20, 21] – their transparent thermodynamic interpretation [22]. However, it has also frequently been noted that in particular the involved secular approximation may lead to strong artifacts [23, 24]. An intuitive explanation for this is that the level spacing in the extended (Floquet) space may become very small, which conflicts with the secular approximation [25]. Therefore, traditional Floquet-LGKS approaches have been questioned in many works [23, 26].

Already for undriven systems, it can be argued that

the (non-LGKS) Redfield equation applied in the proper regime only leads to small violations of density matrix properties in trade for a closer description of physical reality [27]. As a practical benefit, improper density matrices can then be used as an indicator for leaving the region of validity of such perturbative schemes, whereas such a witness is missing for LGKS-based approaches.

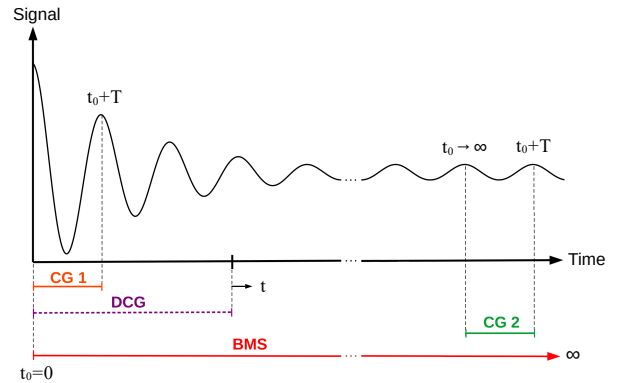


FIG. 1. Sketch illustrating the different coarse-graining timescales to derive a master equation in the weak coupling limit. For CG1 (orange) and CG2 (green) the coarse-graining extends over one period of the driving field $\tau = T$, where for CG1 $t_0 = 0$ and for CG2 the initial coarse-graining time is taken to infinity $t_0 \rightarrow \infty$. For dynamical coarse-graining (DCG) (purple) the coarse-graining time is chosen dynamically as the physical time. For $\tau \rightarrow \infty$ all methods recover the Born-Markov-secular (BMS) limit (red).

Another viewpoint therefore is to preserve the formal GKSL form of the generator while improving in some ways the involved approximations [28]. There are various routes to achieve this, e.g. formally restoring the LGKS form by discarding its subspace with negative eigenvalues [29, 30], by performing only a partial secular approximation [31, 32], or by taking the effects of the reservoir on the direction of the system pointer basis into account [33, 34]. While these approaches apply to undriven systems, we would like to focus on an approach that can be easily combined with periodic driving. Such an approach that can also be well-motivated using a microscopic derivation is the temporal coarse-graining approach [27, 35–46]. Intuitively, it can be understood as

* gernot.schaller@tu-berlin.de

an approximate representation of the reduced exact solution over an appropriately chosen coarse-graining time interval. The freedom in choosing the coarse-graining interval is exemplified in Fig. 1 and shall be the subject of this paper with a focus on periodically driven systems. We begin with a brief introduction into the method in Sec. II and then compare various dissipators for three examples of driven open systems in Secs. III, IV, and V.

II. COARSE-GRAINING METHODS FOR PERIODICALLY DRIVEN OPEN SYSTEMS

The starting point of our considerations is a representation of the Hamiltonian of the full universe in the form

$$H(t) = H_S(t) + \sum_{\alpha} A_{\alpha} \otimes B_{\alpha} + H_B \quad (1)$$

with periodically driven system Hamiltonian $H_S(t + T) = H_S(t)$, (not necessarily individually Hermitian) system and bath coupling operators A_{α} and B_{α} , respectively, and reservoir Hamiltonian H_B . Since system and bath operators act on different Hilbert spaces, we assume from the beginning that $[H_S, H_B] = 0$ and also $[A_{\alpha}, B_{\beta}] = 0$. In an interaction picture with respect to $H_0 = H_S(t) + H_B$ (bold symbols), we can formally solve the von-Neumann equation

$$\dot{\rho} = -i \left[\sum_{\alpha} \mathbf{A}_{\alpha}(t) \otimes \mathbf{B}_{\alpha}(t), \rho \right] \quad (2)$$

by employing the time-evolution operator from time t_0 to time $t_0 + \tau$

$$\rho(t_0 + \tau) = \mathbf{U}(t_0 + \tau, t_0) \rho(t_0) \mathbf{U}^{\dagger}(t_0 + \tau, t_0). \quad (3)$$

The coarse-graining approach originates from the attempt to match the reduced evolution of an open quantum system with a time-local master equation

$$e^{\mathcal{L}\tau} \rho_S^0 \stackrel{!}{=} \text{Tr}_B \{ \mathbf{U}(t_0 + \tau, t_0) \rho_S^0 \otimes \rho_B^0 \mathbf{U}^{\dagger}(t_0 + \tau, t_0) \}. \quad (4)$$

Here, we have already put an index \mathcal{L}_{τ} to the dissipation superoperator to highlight the fact that with a constant \mathcal{L} superoperator it will in general not be possible to capture the exact reduced dynamics for all times, which would require a Kraus representation [47]. For weak system-reservoir interaction (or small propagation times τ) we can use that $\mathbf{U}(t_0 + \tau, t_0)$ is close to the identity and \mathcal{L}_{τ} is small. One can then expand the expressions on both sides and assuming furthermore that $\text{Tr} \{ B_{\alpha} \rho_B^0 \} = 0$, one has a defining equation for the

coarse-graining generator

$$\begin{aligned} \mathcal{L}_{\tau} \rho_S = & -i \frac{1}{2i\tau} \int_{t_0}^{t_0+\tau} dt_1 dt_2 \sum_{\alpha\bar{\alpha}} C_{\alpha\bar{\alpha}}(t_1, t_2) \\ & \times \text{sgn}(t_1 - t_2) [\mathbf{A}_{\alpha}(t_1) \mathbf{A}_{\bar{\alpha}}(t_2), \rho_S] \\ & + \frac{1}{\tau} \int_{t_0}^{t_0+\tau} dt_1 dt_2 \sum_{\alpha\bar{\alpha}} C_{\alpha\bar{\alpha}}(t_1, t_2) \\ & \times \left[\mathbf{A}_{\bar{\alpha}}(t_2) \rho_S \mathbf{A}_{\alpha}(t_1) - \frac{1}{2} \{ \mathbf{A}_{\alpha}(t_1) \mathbf{A}_{\bar{\alpha}}(t_2), \rho_S \} \right], \end{aligned} \quad (5)$$

with bath correlation functions $C_{\alpha\bar{\alpha}}(t_1, t_2) = \text{Tr}_B \{ \mathbf{B}_{\alpha}(t_1) \mathbf{B}_{\bar{\alpha}}(t_2) \rho_B^0 \} = \text{Tr} \{ \mathbf{B}_{\alpha}(\mathbf{t}_1 - \mathbf{t}_2) B_{\beta} \rho_B^0 \}$, where the last equality holds when $[H_B, \rho_B^0] = 0$.

Here, the bold symbols denote the interaction picture, and for system operators we have $\mathbf{A}(t) = U_S^{\dagger}(t, 0) A U_S(t, 0)$ with $U_S(t, 0) = \mathcal{T} \left\{ e^{-i \int_0^t H_S(t') dt'} \right\}$ and \mathcal{T} denoting the time ordering operator. Particularly, for a periodically driven system it can be expressed as a product of a unitary kick operator $U_{\text{kick}}(t, 0)$ with the period of the driving and the evolution under an effective system Floquet Hamiltonian \bar{H} :

$$\begin{aligned} U_S(t, 0) &= U_{\text{kick}}(t, 0) e^{-i\bar{H}t} \\ U_{\text{kick}}(t, 0) &= U_{\text{kick}}(t + T, 0), \quad U_{\text{kick}}(nT, 0) = \mathbb{1}, \end{aligned} \quad (6)$$

with $n \in \mathbb{Z}$, such that the stroboscopic evolution between full periods is given by the Floquet Hamiltonian $U(nT, 0) = e^{-i\bar{H}nT}$. However, it should be stressed here that the above decomposition is not unique. Introducing the eigenbasis of the Floquet Hamiltonian via $\bar{H} |\bar{a}\rangle = \bar{E}_a |\bar{a}\rangle$, we can see that the time evolution operator remains invariant under the simultaneous transformations $\bar{H} \rightarrow \bar{H} + m\Omega |\bar{a}\rangle \langle \bar{a}|$ and $U_{\text{kick}}(t, 0) \rightarrow U_{\text{kick}}(t, 0) e^{+im\Omega t |\bar{a}\rangle \langle \bar{a}|}$, which maintains the periodicity of the kick operator. This gauge degree of freedom allows one to deliberately choose the convention that all eigenenergies of the Floquet Hamiltonian should lie in the first Brillouin zone $\bar{E}_a \in [-\Omega/2, +\Omega/2)$.

Hence, the system coupling operators in the interaction picture $\mathbf{A}_{\alpha}(t)$ can be expressed as:

$$\begin{aligned} \mathbf{A}_{\alpha}(t) &= U_S^{\dagger}(t) A_{\alpha} U_S(t) = e^{i\bar{H}t} U_{\text{kick}}^{\dagger}(t) A_{\alpha} U_{\text{kick}}(t) e^{-i\bar{H}t} \\ &= \sum_{n=-\infty}^{+\infty} e^{i\bar{H}t} \hat{A}_{\alpha}^n e^{in\Omega t} e^{-i\bar{H}t}, \end{aligned} \quad (7)$$

where due to the periodicity of the kick operator we have expanded $U_{\text{kick}}^{\dagger}(t) A_{\alpha} U_{\text{kick}}(t)$ in a Fourier series

$$\hat{A}_{\alpha}^n = \frac{\Omega}{2\pi} \int_{-T/2}^{T/2} U_{\text{kick}}^{\dagger}(t) A_{\alpha} U_{\text{kick}}(t) e^{-in\Omega t} dt, \quad T = \frac{2\pi}{\Omega}. \quad (8)$$

Now, in the eigenbasis of the Floquet Hamiltonian we can also write this as

$$\begin{aligned}
\mathbf{A}_\alpha(t_1) &= \sum_{ab} \sum_n \langle \bar{a} | \hat{A}_\alpha^n | \bar{b} \rangle e^{i(\bar{E}_a - \bar{E}_b + n\Omega)t_1} |\bar{a}\rangle \langle \bar{b}| \\
&\equiv \sum_{ab} \sum_n A_{\alpha,ab}^{+n} e^{i(\bar{E}_a - \bar{E}_b + n\Omega)t_1} L_{ab}, \\
\mathbf{A}_{\bar{\alpha}}(t_2) &= \sum_{cd} \sum_{n'} \langle \bar{c} | \hat{A}_{\bar{\alpha}}^{n'} | \bar{d} \rangle e^{i(\bar{E}_c - \bar{E}_d + n'\Omega)t_2} |\bar{c}\rangle \langle \bar{d}| \\
&\equiv \sum_{cd} \sum_{n'} A_{\bar{\alpha},dc}^{-n'} e^{-i(\bar{E}_c - \bar{E}_d + n'\Omega)t_2} L_{dc}, \quad (9)
\end{aligned}$$

where $L_{ab} \equiv |\bar{a}\rangle \langle \bar{b}|$.

Additionally, the reservoir correlation functions for reservoir at equilibrium depend only on the difference of time arguments, and we can introduce their even and odd Fourier transforms

$$\begin{aligned}
C_{\alpha\bar{\alpha}}(t_1 - t_2) &= \frac{1}{2\pi} \int d\omega \gamma_{\alpha\bar{\alpha}}(\omega) e^{-i\omega(t_1 - t_2)}, \\
C_{\alpha\bar{\alpha}}(t_1 - t_2) \text{sgn}(t_1 - t_2) &= \frac{1}{2\pi} \int d\omega \sigma_{\alpha\bar{\alpha}}(\omega) e^{-i\omega(t_1 - t_2)}. \quad (10)
\end{aligned}$$

The temporal integrals can be analytically performed leading to

$$\begin{aligned}
f_{t_0}^\tau(\alpha, \beta, \omega) &\equiv \frac{1}{2\pi\tau} \int_{t_0}^{t_0+\tau} \int_{t_0}^{t_0+\tau} e^{-i\omega(t_1 - t_2)} e^{i\alpha t_1} e^{-i\beta t_2} dt_1 dt_2 \\
&= \frac{\tau}{2\pi} e^{i(\alpha - \beta)t_0} e^{i(\alpha - \beta)\tau/2} \text{sinc}\left[(\alpha - \omega)\frac{\tau}{2}\right] \\
&\quad \times \text{sinc}\left[(\beta - \omega)\frac{\tau}{2}\right]. \quad (11)
\end{aligned}$$

In particular, for discrete α and β one finds that

$$\lim_{\tau \rightarrow \infty} f_{t_0}^\tau(\alpha, \beta, \omega) = \delta_{\alpha\beta} \delta(\alpha - \omega). \quad (12)$$

Inserting it all, we can generally write the dissipator as

$$\dot{\rho}_S = -i[\mathbf{H}_{\text{LS}}^\tau, \rho_S] + \mathcal{D}^\tau \rho_S \quad (13)$$

with the single-integral expressions

$$\begin{aligned}
\mathbf{H}_{\text{LS}}^\tau &= \int d\omega \sum_{\alpha\bar{\alpha}} \sigma_{\alpha\bar{\alpha}}(\omega) \frac{1}{2i} \sum_{nn'} \sum_{abcd} \\
&\quad \times f_{t_0}^\tau(\bar{E}_a - \bar{E}_b + n\Omega, \bar{E}_c - \bar{E}_d + n'\Omega, \omega) \\
&\quad \times A_{\alpha,ab}^n A_{\bar{\alpha},dc}^{-n'} L_{ab} L_{dc}, \\
\mathcal{D}^\tau \rho_S &= \int d\omega \sum_{\alpha\bar{\alpha}} \gamma_{\alpha\bar{\alpha}}(\omega) \sum_{nn'} \sum_{abcd} \\
&\quad \times f_{t_0}^\tau(\bar{E}_a - \bar{E}_b + n\Omega, \bar{E}_c - \bar{E}_d + n'\Omega, \omega) \\
&\quad \times A_{\alpha,ab}^{+n} A_{\bar{\alpha},dc}^{-n'} \\
&\quad \times \left[L_{dc} \rho_S L_{ab} - \frac{1}{2} \{L_{ab} L_{dc}, \rho_S\} \right]. \quad (14)
\end{aligned}$$

Here, the first term defines a (Hermitian) correction to the system Hamiltonian (which for large τ converges to the LGKS Lambshift term), and the second term denotes the dissipative influence of the reservoir.

Since by convention we chose the quasienergies in the first Brillouin zone $\bar{E}_a \in [-\Omega/2, +\Omega/2)$, it follows that the derived energy differences are bounded $\bar{E}_a - \bar{E}_b \in (-\Omega, +\Omega)$. The important observation so far is that for any choice of t_0 and τ , the coarse-graining scheme always yields LGKS-type dissipators [48]. Nevertheless, the different coarse-graining schemes sketched in Fig. 1 may lead to different dissipators. For later reference, we coin the coarse-graining schemes *dynamical coarse-graining* [37] (DCG) with $t_0 = 0$ and $\tau = t$, *initial period-coarse-graining* (CG1) with $t_0 = 0$ and $\tau = T$, *long-term period-coarse-graining* with $t_0 \rightarrow \infty$ and $\tau = T$ (CG2).

Finally, we would like to address the limit of very large coarse-graining times. Technically, this limit allows – based on Eq. (12) – to eliminate the remaining integration

$$\begin{aligned}
\mathbf{H}_{\text{LS}}^\infty &= \frac{1}{2i} \sum_{\alpha\bar{\alpha}} \sum_{nn'} \sum_{abcd} \sigma_{\alpha\bar{\alpha}}(\bar{E}_a - \bar{E}_b + n\Omega) \\
&\quad \times \delta_{\bar{E}_a - \bar{E}_b + n\Omega, \bar{E}_c - \bar{E}_d + n'\Omega} A_{\alpha,ab}^n A_{\bar{\alpha},dc}^{-n'} L_{ab} L_{dc}, \\
\mathcal{D}^\infty \rho_S &= \sum_{\alpha\bar{\alpha}} \sum_{nn'} \sum_{abcd} \gamma_{\alpha\bar{\alpha}}(\bar{E}_a - \bar{E}_b + n\Omega) \\
&\quad \times \delta_{\bar{E}_a - \bar{E}_b + n\Omega, \bar{E}_c - \bar{E}_d + n'\Omega} A_{\alpha,ab}^{+n} A_{\bar{\alpha},dc}^{-n'} \\
&\quad \times \left[L_{dc} \rho_S L_{ab} - \frac{1}{2} \{L_{ab} L_{dc}, \rho_S\} \right]. \quad (15)
\end{aligned}$$

The evaluation of the resonance condition resulting from the Kronecker- δ

$$\bar{E}_a - \bar{E}_b + n\Omega = \bar{E}_c - \bar{E}_d + n'\Omega \quad (16)$$

however requires some care. The typical argument is that for fast driving, the above resonance can only be met if separately $n' = n$ and $\bar{E}_a - \bar{E}_b = \bar{E}_c - \bar{E}_d$. However, the applicability of this argument critically depends on the Floquet spectrum. If for a two-level system we by chance have Floquet energies well within the first Brillouin zone $\bar{E}_a \in \{-\Omega/4, +\Omega/4\}$, this generates energy differences $\bar{E}_a - \bar{E}_b \in \{-\Omega/2, 0, +\Omega/2\}$. In this case, the above resonance condition can also be met with $\bar{E}_a - \bar{E}_b = +\Omega/2$, $\bar{E}_c - \bar{E}_d = -\Omega/2$ and $n' = n + 1$, demonstrating that in general, the long-term limit of periodically driven coarse-graining master equation need not coincide with the significantly simpler Floquet-BMS master equation that results from demanding the resonance separately (i.e., by setting

$$n' = n \text{ and } \bar{E}_a - \bar{E}_b = \bar{E}_c - \bar{E}_d)$$

$$\begin{aligned} \mathbf{H}_{\text{LS}}^{\text{BMS}} &= \frac{1}{2i} \sum_{\alpha\bar{\alpha}} \sum_n \sum_{abcd} \sigma_{\alpha\bar{\alpha}} (\bar{E}_a - \bar{E}_b + n\Omega) \\ &\quad \times \delta_{\bar{E}_a - \bar{E}_b, \bar{E}_c - \bar{E}_d} A_{\alpha,ab}^n A_{\bar{\alpha},dc}^{-n} L_{ab} L_{dc}, \\ \mathcal{D}^{\text{BMS}} \rho_S &= \sum_{\alpha\bar{\alpha}} \sum_n \sum_{abcd} \gamma_{\alpha\bar{\alpha}} (\bar{E}_a - \bar{E}_b + n\Omega) \\ &\quad \times \delta_{\bar{E}_a - \bar{E}_b, \bar{E}_c - \bar{E}_d} A_{\alpha,ab}^{+n} A_{\bar{\alpha},dc}^{-n} \\ &\quad \times \left[L_{dc} \rho_S L_{ab} - \frac{1}{2} \{L_{ab} L_{dc}, \rho_S\} \right]. \quad (17) \end{aligned}$$

Even then, we note that the remaining Kronecker- δ leaves many terms that are often neglected. For example, the above resonance can always be trivially fulfilled with $\bar{E}_a = \bar{E}_b$ and $\bar{E}_c = \bar{E}_d$, even for the undriven case. For many models, one has that $\gamma_{\alpha\bar{\alpha}}(0) \rightarrow 0$, such that such terms would not contribute anyways for undriven systems, where $\Omega \rightarrow 0$. But in general they will have to be kept. For comparison we therefore also state the ultra-secular approximation (BMU), where only terms with $a = c$ and $b = d$ are kept

$$\begin{aligned} \mathbf{H}_{\text{LS}}^{\text{BMU}} &= \frac{1}{2i} \sum_{\alpha\bar{\alpha}} \sum_n \sum_{ab} \sigma_{\alpha\bar{\alpha}} (\bar{E}_a - \bar{E}_b + n\Omega) \\ &\quad \times A_{\alpha,ab}^n A_{\bar{\alpha},ba}^{-n} L_{ab} L_{ba}, \\ \mathcal{D}^{\text{BMU}} \rho_S &= \sum_{\alpha\bar{\alpha}} \sum_n \sum_{ab} \gamma_{\alpha\bar{\alpha}} (\bar{E}_a - \bar{E}_b + n\Omega) A_{\alpha,ab}^{+n} A_{\bar{\alpha},ba}^{-n} \\ &\quad \times \left[L_{ba} \rho_S L_{ab} - \frac{1}{2} \{L_{ab} L_{ba}, \rho_S\} \right]. \quad (18) \end{aligned}$$

In what follows, we will compare the solutions to various periodically driven problems that are based on these different coarse-graining approaches, i.e., for the DCG approach we evaluate Eq. (14) with $\tau = t$ and $t_0 = 0$, for the CG1 approach we use Eq. (14) with $\tau = T$ and $t_0 = 0$, for the CG2 approach we use Eq. (14) with $\tau = T$ and $t_0 \rightarrow \infty$, whereas for the BMS and BMU results we use Eqns. (17) and (18), respectively. Furthermore, in our calculations we will for simplicity neglect the Hermitian correction term to the Hamiltonian $\mathbf{H}_{\text{LS}}^{\text{BMS}}$ throughout. Whereas for the particular pure-dephasing model considered below this term has no effect anyways, in general it can only be neglected in the weak-coupling regime where $|H_{\text{LS}}^{\text{BMS}}| \ll |H_S|$.

III. PURE-DEPHASING MODELS

By the term pure-dephasing models we summarize models where the interaction commutes with the system Hamiltonian at all times, i.e., system and reservoir cannot exchange energy. The Hamiltonian of a general driven-system pure-dephasing model with a reservoir of

bosonic oscillators is then given by:

$$\begin{aligned} H(t) &= H_S(t) + A \otimes \sum_k \left(h_k b_k + h_k^* b_k^\dagger \right) + \sum_k \omega_k b_k^\dagger b_k, \\ [H_S(t), A] &= 0. \end{aligned} \quad (19)$$

The assumption of commuting coupling operator A and system Hamiltonian $H_S(t)$ allows to solve the dynamics exactly.

A. Exact solution

Specifically for a driven two level system with $H_S = \sigma^z [\frac{\Delta}{2} + \lambda \cos(\Omega t)]$ and coupling $A = \sigma^z$ we obtain that the populations in the σ^z eigenbasis remain constant

$$\rho_{S,00}(t) = \rho_{S,00}^0, \quad \rho_{S,11}(t) = \rho_{S,11}^0, \quad (20)$$

whereas the coherences evolve according to

$$\begin{aligned} \rho_{S,10}(t) &= e^{+2i(\frac{\Delta}{2}t + \frac{\lambda}{\Omega} \sin(\Omega t))} \\ &\quad \times \exp \left\{ -\frac{4}{\pi} \int_{-\infty}^{\infty} d\omega \gamma(\omega) \frac{\sin^2(\frac{\omega t}{2})}{\omega^2} \right\} \rho_{S,10}^0. \end{aligned} \quad (21)$$

compare App. A. Here, $\gamma(\omega) = \Gamma(\omega)[1 + n_B(\omega)]$ with spectral density $\Gamma(\omega) \equiv 2\pi \sum_k |h_k|^2 \delta(\omega - \omega_k)$ (analytically continued via $\Gamma(-\omega) = -\Gamma(\omega)$ to the complete real axis) and Bose distribution $n_B(\omega) = [e^{\beta\omega} - 1]^{-1}$. In absence of driving ($\lambda \rightarrow 0$), this falls back to the known pure-dephasing solution of the spin-boson model, see e.g. Ref. [36].

B. Master equation solutions

We can now compare this exact solution with the various approximate approaches discussed before by identifying the single coupling operator $A_1 = \sigma^z$. Particularly, with an odd spectral density, the Fourier transform of the only reservoir correlation function becomes $\gamma_{11}(\omega) = \Gamma(\omega)[1 + n_B(\omega)]$ and the matrix elements of the coupling operators become rather trivial $A_{\alpha,ab}^n = \delta_{\alpha,1} \delta_{n,0} \delta_{ab} \langle \bar{a} | \sigma^z | \bar{a} \rangle$. To compute them, it suffices to realize that for this simple problem the system Floquet Hamiltonian is just $\bar{H} = \frac{\Delta}{2} \sigma^z$, such that its eigenstates are trivial.

C. Comparison

We analytically find that the DCG approach (adaptively choosing $\tau = t$ and $t_0 = 0$ in Eq. (14)) reproduces the exact solution. Furthermore, we also analytically find that CG1 and CG2 approaches ($\tau = T$ in E. 14)) both agree for this model class. We also find analytically

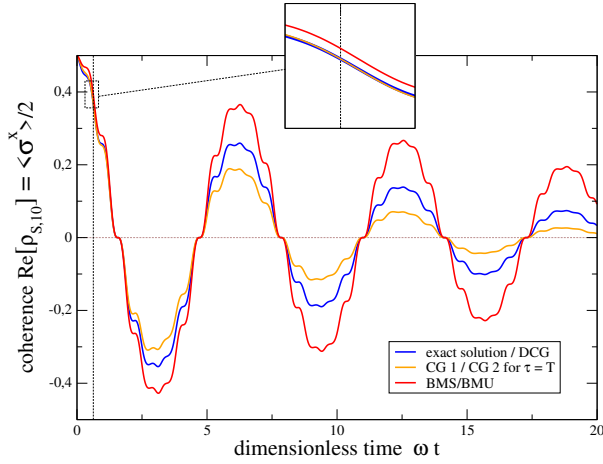


FIG. 2. Plot of $\langle \sigma^x \rangle / 2$ comparing coarse-graining CG1/2 for $\tau = T = \frac{2\pi}{\Omega}$ (yellow) and the BMS/BMU solution (red) to the exact analytical solution (blue). Here, CG1 and CG2 as well as BMS and BMU solutions are identical, whereas DCG ($\tau = t$) reproduces the exact solution. By construction, CG1/CG2 (yellow) and DCG solutions (blue) intersect at $t = T$ (vertical dashed line). Parameters: $\Omega = 10 \Delta$, $\lambda = \frac{1}{2} \Delta$, $\Gamma(\omega) = \Gamma_0 \omega e^{-|\omega|/\omega_c}$ with $\Gamma_0 = 0.05$, $\omega_c = 20 \Delta$, $\beta \Delta = 1$, $\rho_S^0 = 1/2(\mathbf{1} + \sigma^x)$.

from the trivial structure of the model that BMS (17) and BMU (18) solutions must coincide. In Fig. 2 one can see that an additional driving modifies the decay of coherences by super-imposing additional oscillations. Apart from that, we see that the exact reduced dynamics cannot be reproduced by a single Markovian generator (like CG1, CG2, BMS or BMU). However, since pure-dephasing-type models are a very specific model class, we consider models that allow the exchange of energy between system and reservoir below.

IV. CIRCULAR DRIVING

As a second model, we consider a periodically driven open two level system of the form

$$H(t) = \frac{\Delta}{2} \sigma^z + P \sigma^+ e^{-i\Omega t} + P^* \sigma^- e^{+i\Omega t} + \sum_k (\sigma^+ h_k b_k + \sigma^- h_k^* b_k^\dagger) + \sum_k \omega_k b_k^\dagger b_k, \quad (22)$$

where P denotes a driving amplitude. In absence of driving and for a vacuum reservoir, the model is exactly solvable [7], but we are here interested in the case of finite driving amplitudes but weak system-reservoir coupling. By employing the unitary transform

$$V(t) = \exp \left[-i \left(\frac{\Omega t}{2} \sigma^z + \Omega t \sum_k b_k^\dagger b_k \right) \right] \quad (23)$$

one can see from the observations

$$\begin{aligned} V^\dagger(t) \sigma^z V(t) &= \sigma^z, & V^\dagger(t) \sigma^\pm V(t) &= \sigma^\pm e^{\pm i\Omega t}, \\ V^\dagger(t) b_k V(t) &= e^{-i\Omega t} b_k, & V^\dagger(t) b_k^\dagger V(t) &= e^{+i\Omega t} b_k^\dagger, \end{aligned} \quad (24)$$

that the total Hamiltonian becomes time-independent under the gauge transformation

$$\begin{aligned} V^\dagger(t) H(t) V(t) &= \frac{\Delta}{2} \sigma^z + P \sigma^+ + P^* \sigma^- \\ &+ \sum_k (\sigma^+ h_k b_k + \sigma^- h_k^* b_k^\dagger) + \sum_k \omega_k b_k^\dagger b_k. \end{aligned} \quad (25)$$

Accordingly, by transforming into the corresponding picture, the expectation value of an observable O can be written as

$$\langle O \rangle = \text{Tr} \{ O U(t) \rho_0 U^\dagger(t) \} \equiv \text{Tr} \{ \tilde{O}(t) \tilde{U}(t) \rho_0 \tilde{U}^\dagger(t) \} \quad (26)$$

with the effective time evolution operator $\tilde{U}(t) = V^\dagger(t) U(t)$ and transformed observable $\tilde{O}(t) = V^\dagger(t) O V(t)$. The effective time evolution operator evolves according to a time-independent picture

$$\begin{aligned} \frac{d}{dt} \tilde{U}(t) &= -i \tilde{H} \tilde{U}(t), \\ \tilde{H} &= V^\dagger(t) H(t) V(t) + i \dot{V} V \\ &= \frac{\Delta - \Omega}{2} \sigma^z + P \sigma^+ + P^* \sigma^- \\ &+ \sum_k (\sigma^+ h_k b_k + \sigma^- h_k^* b_k^\dagger) + \sum_k (\omega_k - \Omega) b_k^\dagger b_k, \end{aligned} \quad (27)$$

such that we can write $\tilde{U}(t) = e^{-i\tilde{H}t}$.

A. Benchmark solution

Therefore, under the gauge transform (25), the time evolution is just that of a time-independent open two-level system. In this picture, we can set up the Born-Markov secular approximations and derive the BMS master equation for an undriven system. Formally, this looks like Eq. (17) with keeping only the $n = 0$ term and instead of the Floquet Hamiltonian eigenstates and eigenvalues using the eigenstates and eigenvalues of $\tilde{H}_S = \frac{\Delta - \Omega}{2} \sigma^z + P \sigma^+ + P^* \sigma^-$. Due to a shifted KMS relation, this master equation does not thermalize even in the time-independent picture but reaches some nonequilibrium steady state, which – after transforming back to the original picture – exhibits a time-dependence with the period of the driving.

In the long-term limit, we can apply an even simpler analysis: For non-degenerate eigenvalues of the effective system Hamiltonian \tilde{H}_S , the populations decouple from the coherences and the evolution is given

by a simple rate equation: $\dot{\tilde{\rho}}_{S,aa} = \sum_b \gamma_{ab,ab} \tilde{\rho}_{S,bb} - \sum_b \gamma_{ba,ba} \tilde{\rho}_{S,aa}$ with transition rates from energy level b to a given by $\gamma_{ab,ab}$. The steady state solution is then given by

$$\begin{aligned} \tilde{\rho}_S &= P_- |-\rangle \langle -| + (1 - P_-) |+\rangle \langle +|, \\ P_- &= \frac{\gamma_{-+, -+}}{\gamma_{-+, -+} + \gamma_{+-, +-}}, \end{aligned} \quad (28)$$

where $|-\rangle$ and $|+\rangle$ denote the ground and excited state of \tilde{H}_S , respectively. For our example the two transition rates read

$$\begin{aligned} \gamma_{-+, -+} &= \tilde{\gamma}_{12}(E_+ - E_-) |\langle - | \sigma^- | + \rangle|^2 \\ &\quad + \tilde{\gamma}_{21}(E_+ - E_-) |\langle - | \sigma^+ | + \rangle|^2, \\ \gamma_{+-, +-} &= \tilde{\gamma}_{12}(E_- - E_+) |\langle + | \sigma^- | - \rangle|^2 \\ &\quad + \tilde{\gamma}_{21}(E_- - E_+) |\langle + | \sigma^+ | - \rangle|^2, \end{aligned} \quad (29)$$

with $\tilde{\gamma}_{12}(\omega) = \Theta(\omega + \Omega) \Gamma(\omega + \Omega) [1 + n_B(\omega + \Omega)]$ and $\tilde{\gamma}_{21}(\omega) = \Theta(-\omega + \Omega) \Gamma(-\omega + \Omega) n_B(-\omega + \Omega)$ exemplifying the broken Kubo-Martin-Schwinger [49–51] relation $\frac{\tilde{\gamma}_{21}(-\omega)}{\tilde{\gamma}_{12}(\omega)} = e^{-\beta(\omega + \Omega)}$. In this picture, system observables can be computed via

$$\langle O \rangle \rightarrow \text{Tr}_S \left\{ e^{+i\Omega t/2\sigma^z} O e^{-i\Omega t/2\sigma^z} \tilde{\rho}_S(t) \right\}, \quad (30)$$

where for large times we can insert $\tilde{\rho}(t) \rightarrow \tilde{\rho}_S$ as given by Eq. (28).

The blue curves in Figs. 3 and 4 provide the full time-dependent BMS solution in the time-independent picture, which in the long-term limit coincides with the limit discussed above.

B. Master equation solutions

We now go back to the original Schrödinger picture representation of Eq. (22), where we can identify system coupling operators $A_1 = \sigma^+$ and $A_2 = \sigma^-$. Additionally, the non-vanishing correlation functions become $\gamma_{12}(\omega) = \Theta(\omega) \Gamma(\omega) [1 + n_B(\omega)]$ and $\gamma_{21}(\omega) = \Theta(-\omega) \Gamma(-\omega) n_B(-\omega)$. Furthermore, one finds that kick-operator and Floquet Hamiltonian are given by

$$\begin{aligned} \bar{H} &= \frac{\Delta - \Omega}{2} \sigma^z + P \sigma^+ + P^* \sigma^- - \frac{\Omega}{2} \mathbf{1}, \\ U_{\text{kick}}(t, 0) &= \exp \left(-i \frac{\Omega t}{2} (\mathbf{1} + \sigma^z) \right). \end{aligned} \quad (31)$$

This allows us to compute the coarse-graining dissipators CG1, CG2, and DCG as well as BMS and BMU dissipators.

C. Comparison

We compare the resulting dynamics with the previously discussed asymptotic solution in Figs. 3 and 4.

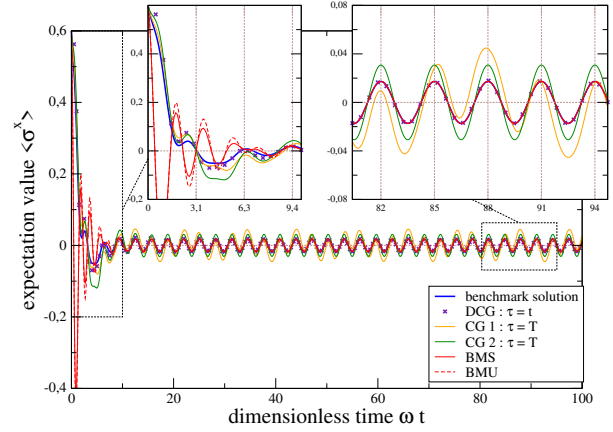


FIG. 3. Plot of the time-dependent expectation value of Pauli matrix σ^x according to the asymptotic solution in the time independent frame from Eq. (30) (blue), CG1 (orange), CG2 (green), BMS/BMU (red/red dashed) and DCG (purple crosses). The gridlines mark multiples of the driving period T . At long times, all DCG, BMS, and BMU solutions all show a perfect numerical agreement with the long-term benchmark solution (right inset). For short times, the DCG solution agrees better with the benchmark than the BMS and BMU solutions, which also differ from each other then (left inset). Parameters: $\Omega = 2 \Delta$, $P = \frac{1}{2} \Delta$ (with Floquet energies ($\bar{E}_{\pm} = \pm \frac{2-\sqrt{2}}{2} \Delta$) in the first Brillouin zone), $\beta \Delta = 0.1$, $\Gamma_0 = 0.05$, $\omega_c = 15 \Delta$, $\rho_S^0 = 1/2[\mathbf{1} + 0.6\sigma^x + 0.4\sigma^z]$.

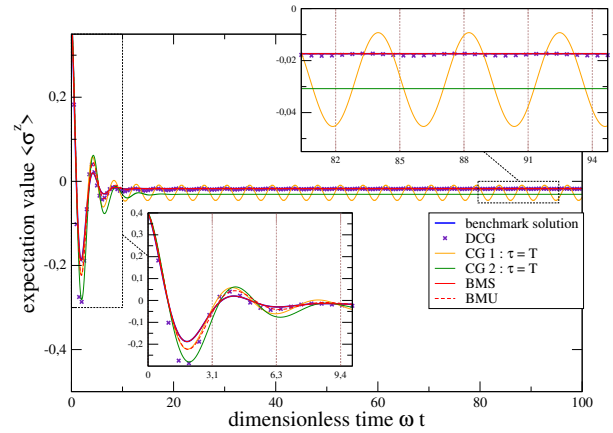


FIG. 4. Plot of the time-dependent expectation value of Pauli matrix σ^z . By construction, for short times the DCG solution is superior to the other perturbative methods, but again DCG, BMS, and BMU solution converge to the steady-state long-term solution for large times. Color coding and parameters identical to Fig. 3.

Again, we see a convincing agreement of the DCG approach with the steady-state benchmark solution (blue) in the long-time limit, but in this limit, the computationally much simpler BMS and BMU approaches perform equally well. Here one finds strong differences only transiently, where for short times the DCG approach by construction will approximate the exact solution and must therefore also be close to the benchmark solution

for the chosen parameters.

V. FAST-DRIVING SOLUTION

As a last example, we consider systems where the driving breaks the pure-dephasing character of the system

$$H(t) = H_S^0 + \lambda \cos(\Omega t) C + A \otimes \sum_k (h_k b_k + h_k^* b_k^\dagger) + \sum_k \omega_k b_k^\dagger b_k, \quad (32)$$

with arbitrary system Hamiltonian H_S^0 and system coupling operator $A = A^\dagger$ fulfilling $[H_S^0, A] = 0$ and system driving operator $C = C^\dagger$ with in general $[H_S^0, C] \neq 0$. Under a naive RWA approximation, the contribution of the driving vanishes, and the exact solution from the previous section in absence of driving ($\lambda = 0$) applies for all values of the system-reservoir coupling strength. To go beyond the naive RWA, we transform into an interaction picture with respect to the driving

$$U_1(t) = e^{-i\lambda/\Omega \sin(\Omega t) C}, \quad (33)$$

and in this picture (marked by a tilde e.g. via $\tilde{A}(t) = U_1^\dagger(t) A U_1(t)$) the transformed Hamiltonian assumes a time-dependent pure-dephasing form

$$\tilde{H}(t) = \tilde{H}_S^0(t) + \tilde{A}(t) \otimes \sum_k (h_k b_k + h_k^* b_k^\dagger) + \sum_k \omega_k b_k^\dagger b_k, \quad (34)$$

where we still have $[\tilde{H}_S^0(t), \tilde{A}(t)] = U_1^\dagger(t) [H_S^0, A] U_1(t) = 0$. Nevertheless, we cannot apply the naive polaron treatment of App. A, since now also the coupling operator has picked up a periodic time-dependence. However, depending on the problem one may have the situation that also the time averages of the operators

$$\bar{H}_S^0 \equiv \frac{1}{T} \int_0^T \tilde{H}_S^0(t) dt, \quad \bar{A} \equiv \frac{1}{T} \int_0^T \tilde{A}(t) dt \quad (35)$$

commute with each other $[\bar{H}_S^0, \bar{A}] = 0$, and in this case the Hamiltonian after the RWA in the interaction picture

$$\bar{H}_{\text{tot}} = \bar{H}_S^0 + \bar{A} \otimes \sum_k (h_k b_k + h_k^* b_k^\dagger) + \sum_k \omega_k b_k^\dagger b_k \quad (36)$$

is of pure-dephasing type and can be solved with standard methods, see App. B for details. The transformation into this frame is of course not equivalent to the interaction picture representation. However, under the RWA in this transformed frame, the time evolution operator of the system becomes $U_S(t) \approx U_1(t) e^{-i\bar{H}_S^0 t}$, such that we can identify approximations to kick operator $U_{\text{kick}}(t) \approx U_1(t)$ and system Floquet Hamiltonian $\bar{H} \approx \bar{H}_S^0$, respectively.

A. Fast driving benchmark

Specifically, for a two level system with

$$H_S^0 = \frac{\Delta}{2} \sigma^z, \quad A = \sigma^z, \quad C = \sigma^x, \quad (37)$$

we obtain with the Fourier decomposition

$$\begin{aligned} \tilde{A}(t) &= U_1^\dagger(t) \sigma^z U_1(t) \\ &= \sigma^z \sum_{n=-\infty}^{\infty} \mathcal{J}_{2n} \left(\frac{2\lambda}{\Omega} \right) e^{i2n\Omega t} \\ &\quad - i\sigma^y \sum_{n=-\infty}^{\infty} \mathcal{J}_{2n+1} \left(\frac{2\lambda}{\Omega} \right) e^{i(2n+1)\Omega t} \end{aligned} \quad (38)$$

that this method – under the RWA in the transformed frame – yields the following dynamics

$$\begin{aligned} \langle \sigma^x \rangle &= [\cos(\mu_1 \Delta t) \langle \sigma^x \rangle_0 - \sin(\mu_1 \Delta t) \langle \sigma^y \rangle_0] \Sigma(t), \\ \langle \sigma^y \rangle &= -\sin\left(\frac{2\lambda}{\Omega} \sin(\Omega t)\right) \langle \sigma^z \rangle_0 + \cos\left(\frac{2\lambda}{\Omega} \sin(\Omega t)\right) \\ &\quad \times [\sin(\mu_1 \Delta t) \langle \sigma^x \rangle_0 + \cos(\mu_1 \Delta t) \langle \sigma^y \rangle_0] \Sigma(t), \\ \langle \sigma^z \rangle &= +\cos\left(\frac{2\lambda}{\Omega} \sin(\Omega t)\right) \langle \sigma^z \rangle_0 + \sin\left(\frac{2\lambda}{\Omega} \sin(\Omega t)\right) \\ &\quad \times [\sin(\mu_1 \Delta t) \langle \sigma^x \rangle_0 + \cos(\mu_1 \Delta t) \langle \sigma^y \rangle_0] \Sigma(t), \end{aligned} \quad (39)$$

with $\Sigma(t) = \exp \left\{ -\frac{4}{\pi} (\mu_1)^2 \int_{-\infty}^{\infty} \gamma(\omega) \frac{\sin^2(\frac{\omega t}{2})}{\omega^2} d\omega \right\}$ and

$\mu_1 = \mathcal{J}_0\left(\frac{2\lambda}{\Omega}\right)$ being given by the Bessel function of the first kind [52]. Details on this can be found in App. B by inserting the expressions for a two level system in Eq. (B4). In absence of driving $\lambda \rightarrow 0$ one can check with $\mu_1 \rightarrow 1$ that this falls back to the exact pure-dephasing solution [36, 53] with constant populations and decaying coherences

$$\rho_{00}(t) = \frac{1}{2} (\langle \sigma^z \rangle + 1) \rightarrow \rho_{00}^0, \quad (40)$$

$$\rho_{10}(t) = \langle \sigma^+ \rangle \rightarrow e^{+i\Delta t} e^{-\frac{4}{\pi} \int_{-\infty}^{\infty} d\omega \gamma(\omega) \frac{\sin^2(\frac{\omega t}{2})}{\omega^2}} \rho_{10}^0,$$

as $\mathcal{J}_0\left(\frac{2\lambda}{\Omega}\right) \rightarrow 1$ for $\lambda \rightarrow 0$. Furthermore, at vanishing system-reservoir coupling we have $\Sigma(t) \rightarrow 1$, where one can immediately verify that the purity of an initial state is preserved. Finally, we can see that for reasonable spectral densities we find that $\lim_{t \rightarrow \infty} \Sigma(t) = 0$, such that the long-term asymptotics of (39) is given by

$$\begin{aligned} \langle \sigma^y \rangle &\rightarrow -\sin\left(\frac{2\lambda}{\Omega} \sin(\Omega t)\right) \langle \sigma^z \rangle_0, \\ \langle \sigma^z \rangle &\rightarrow +\cos\left(\frac{2\lambda}{\Omega} \sin(\Omega t)\right) \langle \sigma^z \rangle_0. \end{aligned} \quad (41)$$

Importantly, we stress that the fast-driving solution is valid also for stronger system-reservoir couplings [54].

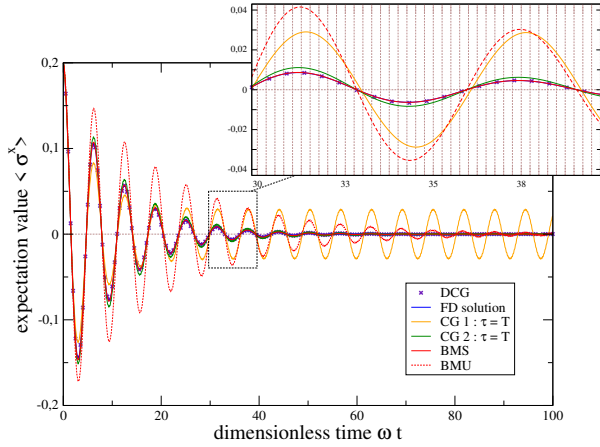


FIG. 5. Plot of the time-dependent expectation value of Pauli matrix σ^x comparing the analytical fast-driving solution (blue), CG1 (yellow), CG2 (green), BMS (red), BMU (red dashed) and DCG (purple cross). The gridlines mark multiples of the driving period T . A higher order approximation for the driving yields similar results (not shown). Parameters: $\Omega = 25 \Delta$, $\lambda = \frac{1}{2} \Delta$, $\beta \Delta = 1$, $\Gamma_0 = 0.05$, $\omega_c = 15 \Delta$, $\rho_0 = 1/2(1 + 0.2\sigma^x + 0.4\sigma^z)$.

B. Master equation solutions

Since we are interested in the fast driving regime here, we consider kick operator $U_{\text{kick}}(t) \approx \exp\{-i\lambda/\Omega \sin(\Omega t)\sigma^x\}$ and system Floquet Hamiltonian $\bar{H} \approx \frac{\Delta}{2}\mathcal{J}_0\left(\frac{2\lambda}{\Omega}\right)\sigma^z$ also by applying the RWA in the transformed frame. Considering the scaling of the Bessel functions at small arguments, we therefore consistently only keep the lowest order terms with $n \in \{-1, 0, +1\}$ in Eq. (38). Then, the coupling operator in the interaction picture can be approximately written as

$$\mathbf{A}_1(t) \approx \mathcal{J}_0\left(\frac{2\lambda}{\Omega}\right)\sigma^z + 2\sin(\Omega t)\mathcal{J}_1\left(\frac{2\lambda}{\Omega}\right)e^{+i\bar{H}t}\sigma^y e^{-i\bar{H}t} + \mathcal{O}\left\{\frac{\lambda^2}{\Omega^2}\right\}, \quad (42)$$

which suffices to set up all master equations. We have numerically checked convergence in the shown parameter regime by considering also the case $n \in \{-2, \dots, +2\}$ (not shown).

C. Comparison

In the limit of both fast driving and weak coupling we can compare the benchmark solution with the perturbative CG1/CG2/DCG/BMS/BMU approaches, which leads to Fig. 5 and Fig. 6.

There, we can observe that the DCG approach performs best. It has however the disadvantage that the generator has to be re-computed for any desired time. Still, all perturbative approaches fail to correctly cap-

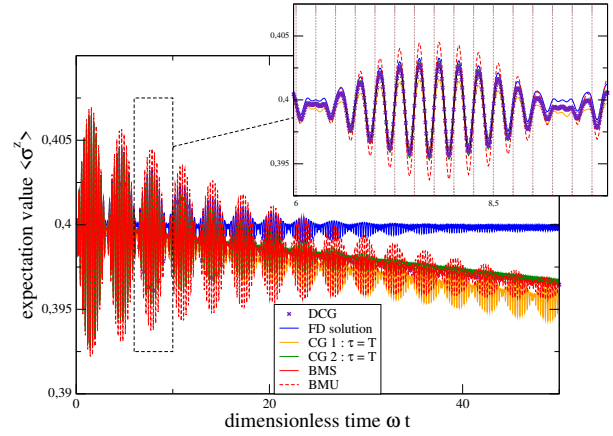


FIG. 6. Plot of the time-dependent expectation value of Pauli matrix σ^z . Color coding and parameters analogous to Fig. 5.

ture the long-term dynamics of the fast-driving solution (39), which is not surprising as the latter is non-perturbative in the system-reservoir coupling strength.

VI. CONCLUSIONS

Our intention in this study was to find an improved but simple (Markovian) master equation applicable to periodically driven systems. For this, we analyzed driven qubit systems coupled to thermal reservoirs with coarse-graining approaches. All methods used had the formal advantage of being in LGKS form.

The negative result is that the analyzed coarse-graining approaches over one period of the driving CG1 and CG2 did not match the expectations, i.e., they were inferior to the DCG approach, even in the special case of pure dephasing. On the positive side, we found that the BMS approach can yield quite reliable results in the long term limit provided the secular approximation is performed in a proper way. The DCG approach performed at least as good as the BMS variant in the long-term limit and approaches the exact solution by construction in the short-term limit, such that we consider it as the most accurate second-order perturbative solution among the schemes tested. Its drawback is the computational cost, since for each time a suitable dissipator needs to be calculated numerically. To avoid this, we note that by using spectral densities with a simpler polynomial structure, the involved integrals in (14) can be performed analytically. The fact that it is not possible to capture the full dynamics faithfully with a single coarse-graining time could be taken as a hint that the restriction to LGKS dynamics is too severe such that one should rather aim at deriving Kraus representations from first principles.

ACKNOWLEDGMENTS

R.H. acknowledges financial support by the Japanese Student Services Organization JASSO. G.S. gratefully acknowledges discussions with J. Abelaßmayer, T. Becker, A. Eckardt, and A. Schnell.

Appendix A: Exact pure-dephasing solution

For a driven Hamiltonian of pure dephasing form (19), the exact dynamics can be calculated by using a polaron (or Lang-Firsov [55]) transform:

$$U_p = e^{A \otimes \left(\frac{h_k}{\omega_k} b_k - \frac{h_k^*}{\omega_k} b_k^\dagger \right)}. \quad (\text{A1})$$

Applying this transformation to system and bath operators yields:

$$\begin{aligned} U_p^\dagger H_S(t) U_p &= H_S(t), & U_p^\dagger A U_p &= A, \\ U_p^\dagger b_k U_p &= b_k - \frac{h_k^*}{\omega_k} A, & U_p^\dagger b_k^\dagger U_p &= b_k^\dagger - \frac{h_k}{\omega_k} A, \end{aligned} \quad (\text{A2})$$

which leads to decoupled system and bath Hamiltonians

$$\begin{aligned} U_p^\dagger H(t) U_p &= H_S(t) - \left(\sum_k \frac{|h_k|^2}{\omega_k} \right) A^2 + \sum_k \omega_k b_k^\dagger b_k \\ &\equiv \bar{H}_S(t) + \sum_k \omega_k b_k^\dagger b_k, \end{aligned} \quad (\text{A3})$$

with $\bar{H}_S(t)$ denoting an effective system Hamiltonian. Hence, the time evolution operator in the polaron picture $\tilde{U}(t)$ is given by the system and bath evolution separately

$$\tilde{U}(t) = \mathcal{T} \left\{ e^{-i \int_0^t \bar{H}_S(t') dt'} \right\} e^{-i \sum_k \omega_k b_k^\dagger b_k t}, \quad (\text{A4})$$

where \mathcal{T} denotes the time-ordering operator of the system. For a general unitary transformation $V(t)$, the time evolution operator in the original frame $U(t)$ can be expressed in terms of the time evolution operator in the new frame $\tilde{U}(t)$ as follows:

$$U(t) = V(t) \tilde{U}(t) V^\dagger(0). \quad (\text{A5})$$

Thus, for the polaron transform this relation yields:

$$U(t) = U_p \tilde{U}(t) U_p^\dagger. \quad (\text{A6})$$

From this, the expectation value of any system observable O_S ,

$$\begin{aligned} \langle O_S \rangle &= \text{Tr} \{ (O_S \otimes \mathbf{1}_B) \rho(t) \} \\ &= \text{Tr} \{ U^\dagger(t) (O_S \otimes \mathbf{1}_B) U(t) \rho^0 \}, \end{aligned} \quad (\text{A7})$$

can be calculated as:

$$\langle O_S \rangle = \text{Tr} \left\{ U_p \tilde{U}^\dagger(t) U_p^\dagger (O_S \otimes \mathbf{1}_B) U_p \tilde{U}(t) U_p^\dagger \rho^0 \right\}. \quad (\text{A8})$$

For the example of a two level system,

$$H_S(t) = \frac{\Delta}{2} \sigma^z, \quad A = \sigma^z, \quad (\text{A9})$$

the populations $\rho_{S,00}(t) = \frac{1}{2} \langle \mathbf{1} + \sigma^z \rangle$ and $\rho_{S,11}(t) = \frac{1}{2} \langle \mathbf{1} - \sigma^z \rangle$ are constant as $\mathbf{1}$ and σ^z commute with U_p and $\tilde{U}(t)$:

$$\rho_{S,00}(t) = \rho_{S,00}^0, \quad \rho_{S,11}(t) = \rho_{S,11}^0. \quad (\text{A10})$$

For the coherences $\rho_{01} = \langle \sigma^- \rangle$ and $\rho_{10} = \langle \sigma^+ \rangle$, the calculations are more involved. Using that

$$U_p^\dagger \sigma^\pm U_p = e^{\pm 2 \sum_k \left(\frac{h_k^*}{\omega_k} b_k^\dagger - \frac{h_k}{\omega_k} b_k \right)} \sigma^\pm, \quad (\text{A11})$$

and organising bath and system parts together, one gets

$$\begin{aligned} \langle \sigma^\pm \rangle &= \text{Tr} \left\{ U_p U_B^\dagger(t) e^{\pm 2 \sum_k \left(\frac{h_k^*}{\omega_k} b_k^\dagger - \frac{h_k}{\omega_k} b_k \right)} U_B(t) U_S^\dagger(t) \sigma^\pm \right. \\ &\quad \left. \times U_S(t) U_p^\dagger \rho^0 \right\}, \end{aligned} \quad (\text{A12})$$

with $U_B(t) = e^{-i \sum_k \omega_k b_k^\dagger b_k t}$ and $U_S(t) = e^{-i \left(\frac{\Delta}{2} t + \frac{\lambda}{\Omega} \sin(\Omega t) \right) \sigma^z}$. Now, one can use that

$$\begin{aligned} e^{i \sum_k \omega_k b_k^\dagger b_k t} e^{\pm 2 \sum_k \left(\frac{h_k^*}{\omega_k} b_k^\dagger - \frac{h_k}{\omega_k} b_k \right)} e^{-i \sum_k \omega_k b_k^\dagger b_k t} \\ = e^{\pm 2 \sum_k \left(\frac{h_k^*}{\omega_k} b_k^\dagger e^{i \omega_k t} - \frac{h_k}{\omega_k} b_k e^{-i \omega_k t} \right)}, \\ e^{i x \sigma^z} \sigma^\pm e^{-i x \sigma^z} = e^{\pm 2 i x} \sigma^\pm, \end{aligned} \quad (\text{A13})$$

which leads by inserting the identity $U_p^\dagger U_p = \mathbf{1}$ to:

$$\begin{aligned} \langle \sigma^\pm \rangle &= e^{\pm 2 i \left(\frac{\Delta}{2} t + \frac{\lambda}{\Omega} \sin(\Omega t) \right)} \\ &\quad \times \text{Tr} \left\{ U_p e^{\pm 2 \sum_k \left(\frac{h_k^*}{\omega_k} b_k^\dagger e^{i \omega_k t} - \frac{h_k}{\omega_k} b_k e^{-i \omega_k t} \right)} U_p^\dagger U_p \sigma^\pm U_p^\dagger \rho^0 \right\}. \end{aligned} \quad (\text{A14})$$

Next, the polaron transformation is applied to the system and bath parts separately:

$$\begin{aligned} U_p e^{\pm 2 \sum_k \left(\frac{h_k^*}{\omega_k} b_k^\dagger e^{i \omega_k t} - \frac{h_k}{\omega_k} b_k e^{-i \omega_k t} \right)} U_p^\dagger &= e^{\pm 2 \sum_k \left(\frac{h_k^*}{\omega_k} (b_k^\dagger + \frac{h_k}{\omega_k} \sigma^z) e^{i \omega_k t} - \frac{h_k}{\omega_k} (b_k + \frac{h_k^*}{\omega_k} \sigma^z) e^{-i \omega_k t} \right)} \\ U_p \sigma^\pm U_p^\dagger &= e^{\mp 2 \sum_k \left(\frac{h_k^*}{\omega_k} b_k^\dagger - \frac{h_k}{\omega_k} b_k \right)} \sigma^\pm. \end{aligned} \quad (\text{A15})$$

Separating system and bath parts and inserting the initial condition $\rho^0 = \rho_S^0 \otimes \bar{\rho}_B$ yields

$$\begin{aligned} \langle \sigma^\pm \rangle &= e^{\pm 2 i \left(\frac{\Delta}{2} t + \frac{\lambda}{\Omega} \sin(\Omega t) \right)} \\ &\quad \times \text{Tr} \left\{ e^{\pm 4 i \sum_k \frac{|h_k|^2}{\omega_k^2} \sin(\omega_k t) \sigma^z} \sigma^\pm \rho_S^0 \right\} B_\pm(t), \\ B_\pm(t) &= \text{Tr} \left\{ e^{\pm 2 \sum_k \left(\frac{h_k^*}{\omega_k} b_k^\dagger e^{i \omega_k t} - \frac{h_k}{\omega_k} b_k e^{-i \omega_k t} \right)} \right. \\ &\quad \left. \times e^{\mp 2 \sum_k \left(\frac{h_k^*}{\omega_k} b_k^\dagger - \frac{h_k}{\omega_k} b_k \right)} \bar{\rho}_B \right\}. \end{aligned} \quad (\text{A16})$$

The trace over the bath parts $B_{\pm}(t)$ gives:

$$B_{\pm}(t) = \exp \left\{ \mp 4i \sum_k \frac{|h_k|^2}{\omega_k^2} \sin(\omega_k t) \right\} \quad (\text{A17})$$

$$\times \exp \left\{ -4 \sum_k \frac{|h_k|^2}{\omega_k^2} [1 - \cos(\omega_k t)] [1 + 2n_B(\omega_k)] \right\}.$$

Here, $n_B(\omega_k) = \frac{1}{e^{\beta\omega_k} - 1}$ denotes the Bose distribution. Plugging the expression for $B_{\pm}(t)$ into Eq. (A16) and using

$$\text{Tr} \left\{ e^{\pm 4i \sum_k \frac{|h_k|^2}{\omega_k^2} \sin(\omega_k t) \sigma^z} \sigma^{\pm} \rho_S^0 \right\} = e^{\pm 4i \sum_k \frac{|h_k|^2}{\omega_k^2} \sin(\omega_k t)} \times \text{Tr} \{ \sigma^{\pm} \rho_S^0 \}, \quad (\text{A18})$$

eventually yields for the expectation value of σ^{\pm} :

$$\langle \sigma^{\pm} \rangle(t) = e^{\pm 2i \left(\frac{\Delta}{2} t + \frac{\lambda}{\Omega} \sin(\Omega t) \right)} \quad (\text{A19})$$

$$\times e^{-\frac{\Delta}{\pi} \int_0^{\infty} d\omega \Gamma(\omega) \frac{\sin^2 \left(\frac{\omega t}{2} \right)}{\omega^2} [1 + 2n_B(\omega)]} \langle \sigma^{\pm} \rangle_0,$$

where the spectral coupling density $\Gamma(\omega) = 2\pi \sum_k |h_k|^2 \delta(\omega - \omega_k)$ has been inserted and it has been used that $1 - \cos(\omega t) = 2 \sin^2 \left(\frac{\omega t}{2} \right)$.

Appendix B: Analytic fast-driving approximation

We consider the simplified form of Eq. (32) with $H_S^0 = \frac{\Delta}{2} A$. First, we move into an interaction picture with respect to the driving by performing the transformation $U_1(t) = e^{-i \frac{\lambda}{\Omega} \sin(\Omega t) C}$, which yields after applying the rotating wave approximation:

$$\tilde{H}_{\text{RWA}} = \tilde{A} \left(\frac{\Delta}{2} + \sum_k (h_k b_k + h_k^* b_k^{\dagger}) \right) + \sum_k \omega_k b_k^{\dagger} b_k,$$

$$\tilde{A} = \frac{\Omega}{2\pi} \int_0^{\frac{2\pi}{\Omega}} U_1^{\dagger}(t) A U_1(t) dt. \quad (\text{B1})$$

This is the Hamiltonian of a simple pure dephasing system, see Eq. (19), with time independent system Hamiltonian.

Applying the polaron transform (A1), system and bath part of the Hamiltonian can be decoupled and (A3) becomes

$$H_p = U_p^{\dagger} \tilde{H}_{\text{RWA}} U_p$$

$$= \frac{\Delta}{2} \tilde{A} - \sum_k \frac{|h_k|^2}{\omega_k} \tilde{A}^2 + \sum_k h_k b_k^{\dagger} b_k, \quad (\text{B2})$$

which yields for the time evolution operator in this picture:

$$\tilde{U}(t) \approx e^{-i \left(\frac{\Delta}{2} \tilde{A} - \sum_k \frac{|h_k|^2}{\omega_k} \tilde{A}^2 \right) t} e^{-i \sum_k h_k b_k^{\dagger} b_k t}. \quad (\text{B3})$$

In an analogous way as for the pure dephasing system, we can write the expectation value of an observable as:

$$\langle O_S \rangle = \text{Tr} \left\{ U_p \tilde{U}^{\dagger}(t) U_p^{\dagger} U_1^{\dagger} (O_S \otimes \mathbf{1}_B) U_1 U_p \tilde{U}(t) U_p^{\dagger} \rho^0 \right\}. \quad (\text{B4})$$

For a two level system Eq. (37), we get

$$\tilde{A} = \mathcal{J}_0 \left(\frac{2\lambda}{\Omega} \right) \sigma^z, \quad (\text{B5})$$

with $\mathcal{J}_n(x)$ denoting the Bessel function of first kind [56], which is defined as the solution of the differential equation $x^2 \mathcal{J}_n''(x) + x \mathcal{J}_n'(x) - (z^2 + n^2) \mathcal{J}_n(x) = 0$.

-
- [1] G. Floquet, *Annales scientifiques de l'École Normale Supérieure* **12**, 47 (1883).
 - [2] J. H. Shirley, *Phys. Rev.* **138**, B979 (1965).
 - [3] M. Grifoni and P. Hänggi, *Physics Reports* **304**, 229 (1998).
 - [4] A. Eckardt and E. Anisimovas, *New Journal of Physics* **17**, 093039 (2015).
 - [5] M. Bukov, L. D'Alessio, and A. Polkovnikov, *Advances in Physics* **64**, 139 (2015).
 - [6] U. Weiss, *Quantum Dissipative Systems*, Series of Modern Condensed Matter Physics, Vol. 2 (World Scientific, Singapore, 1993).
 - [7] H.-P. Breuer and F. Petruccione, *The Theory of Open Quantum Systems* (Oxford University Press, 2002).
 - [8] M. Schlosshauer, *Decoherence and the Quantum-To-Classical Transition* (Springer-Verlag Berlin Heidelberg, 2007).
 - [9] S. Chu, *Science* **253**, 861 (1991).
 - [10] S. Rice and M. Zhao, *Optical Control of Molecular Dynamics* (Wiley, 2000).
 - [11] M. Aidelsburger, M. Atala, S. Nascimbène, S. Trotzky, Y.-A. Chen, and I. Bloch, *Applied Physics B* **113**, 1–11 (2013).
 - [12] M. Atala, M. Aidelsburger, M. Lohse, J. T. Barreiro,

- B. Paredes, and I. Bloch, *Nature Physics* **10**, 588–593 (2014).
- [13] G. Jotzu, M. Messer, R. Desbuquois, M. Lebrat, T. Uehlinger, D. Greif, and T. Esslinger, *Nature* **515**, 237–240 (2014).
- [14] G. Lindblad, *Communications in Mathematical Physics* **48**, 119 (1976).
- [15] V. Gorini, A. Kossakowski, and E. C. G. Sudarshan, *Journal of Mathematical Physics* **17**, 821 (1976).
- [16] S. Kohler, T. Dittrich, and P. Hänggi, *Physical Review E* **55**, 300–313 (1997).
- [17] D. Gelbwaser-Klimovsky, R. Alicki, and G. Kurizki, *Physical Review E* **87**, 012140 (2013).
- [18] K. Szczygielski, D. Gelbwaser-Klimovsky, and R. Alicki, *Physical Review E* **87**, 012120 (2013).
- [19] K. Szczygielski, *Journal of Mathematical Physics* **55**, 083506 (2014).
- [20] T. Shirai, T. Mori, and S. Miyashita, *Physical Review E* **91** (2015), 10.1103/physreve.91.030101.
- [21] T. Shirai, J. Thingna, T. Mori, S. Denisov, P. Hänggi, and S. Miyashita, *New Journal of Physics* **18**, 053008 (2016).
- [22] G. B. Cuetara, A. Engel, and M. Esposito, *New Journal of Physics* **17**, 055002 (2015).
- [23] S. Restrepo, S. Böhlring, J. Cerrillo, and G. Schaller, *Phys. Rev. B* **100**, 035109 (2019).
- [24] J. Luo, Y. Yan, H. Wang, J. Hu, X.-L. He, and G. Schaller, *Phys. Rev. B* **101**, 125410 (2020).
- [25] D. W. Hone, R. Ketzmerick, and W. Kohn, *Phys. Rev. E* **79**, 051129 (2009).
- [26] A. Schnell, A. Eckardt, and S. Denisov, *Phys. Rev. B* **101**, 100301 (2020).
- [27] R. Hartmann and W. T. Strunz, *Phys. Rev. A* **101**, 012103 (2020).
- [28] R. S. Whitney, *Journal of Physics A: Mathematical and General* **41**, 175304 (2008).
- [29] G. Kiršanskas, M. Franckić, and A. Wacker, *Phys. Rev. B* **97**, 035432 (2018).
- [30] K. Ptaszyński and M. Esposito, *Phys. Rev. Lett.* **122**, 150603 (2019).
- [31] D. Farina and V. Giovannetti, *Phys. Rev. A* **100**, 012107 (2019).
- [32] M. Cattaneo, G. L. Giorgi, S. Maniscalco, and R. Zamboni, *Phys. Rev. A* **101**, 042108 (2020).
- [33] M. G. Schultz and F. von Oppen, *Physical Review B* **80**, 033302 (2009).
- [34] M. G. Schultz, *Physical Review B* **82**, 155408 (2010).
- [35] B. Vacchini, *Physical Review Letters* **84**, 1374–1377 (2000).
- [36] D. A. Lidar, Z. Bihary, and K. Whaley, *Chemical Physics* **268**, 35–53 (2001).
- [37] G. Schaller and T. Brandes, *Physical Review A* **78** (2008), 10.1103/physreva.78.022106.
- [38] G. Schaller, P. Zedler, and T. Brandes, *Physical Review A* **79**, 032110 (2009).
- [39] F. Benatti, R. Floreanini, and U. Marzolino, *epl* **88** (2009), 10.1209/0295-5075/88/20011.
- [40] F. Benatti, R. Floreanini, and U. Marzolino, *Phys. Rev. A* **81**, 012105 (2010).
- [41] A. Royer, *Physical Review Letters* **77** (1996), 10.1103/PhysRevLett.77.3272.
- [42] R. Karrlein and H. Grabert, *Phys. Rev. E* **55**, 153 (1997).
- [43] G. Schaller, P. Zedler, and T. Brandes, *Phys. Rev. A* **79**, 032110 (2009).
- [44] C. Majenz, T. Albash, H.-P. Breuer, and D. A. Lidar, *Physical Review A* **88**, 012103 (2013).
- [45] A. Rivas, *Physical Review A* **95**, 042104 (2017).
- [46] A. Rivas, *Entropy* (2019), 10.3390/e21080725.
- [47] K. Kraus, *Annals of Physics* **64**, 311 (1971).
- [48] G. Schaller and J. Ablaßmayer, *Entropy* **22**, 525 (2020).
- [49] R. Kubo, *Journal of the Physical Society of Japan* **12**, 570 (1957).
- [50] P. C. Martin and J. Schwinger, *Physical Review* **115**, 1342 (1959).
- [51] A. Kossakowski, A. Frigerio, V. Gorini, and M. Verri, *Communications in Mathematical Physics* **57**, 97 (1977).
- [52] M. Abramowitz and I. A. Stegun, eds., *Handbook of Mathematical Functions* (National Bureau of Standards, 1970).
- [53] A. J. Leggett, S. Chakravarty, A. T. Dorsey, M. P. A. Fisher, A. Garg, and W. Zwerger, *Reviews of Modern Physics* **59**, 1 (1987).
- [54] S. Restrepo, J. Cerrillo, V. M. Bastidas, D. G. Angelakis, and T. Brandes, *Phys. Rev. Lett.* **117**, 250401 (2016).
- [55] I. G. Lang and Y. A. Firsov, *Soviet Physics JETP* **16**, 1301 (1963).
- [56] M. Abramowitz and I. A. Stegun, *Handbook of Mathematical Functions* (National Bureau of Standards, 1970).